Article

Development of Dual-Aptamers for Constructing Sandwich-Type Pancreatic Polypeptide Assay

Shiya Qin, Nandi Chen, Xiaohai Yang, Qing Wang, Kemin Wang, Jin Huang, Jianbo Liu, and Maogui Zhou

ACS Sens., **Just Accepted Manuscript** • DOI: 10.1021/acssensors.6b00836 • Publication Date (Web): 20 Jan 2017

Development of Dual-Aptamers for Constructing Sandwich-Type Pancreatic Polypeptide Assay

Shiya Qin,‡ Nandi Chen,‡ Xiaohai Yang,* Qing Wang, Kemin Wang,* Jin Huang, Jianbo Liu, Maogui Zhou

State Key Laboratory of Chemo/Biosensing and Chemometrics, College of Chemistry and Chemical Engineering, Key Laboratory for Bio-Nanotechnology and Molecular Engineering of Hunan Province, Hunan University, Changsha 410082, China.

KEYWORDS: aptamer, pancreatic polypeptide, graphene oxide, sandwich assay, gold nanoparticle

ABSTRACT: Pancreatic polypeptide (PP) is a specific biomarker of non-functional pancreatic neuroendocrine tumors (NF-pNETs), clinical significance of PP inspires researchers to make great efforts in developing sensitive and specific sensors. However, there is no existing biosensor for detecting PP that combines facility and functionality. Addressing this challenge, a pair of aptamers which could be used to develop sandwich assay for PP is reported. First, several high affinitive aptamers are screened through graphene oxide-based SELEX, and appropriate dual-aptamers which could bind to different epitopes of PP are identified through fluorescence assays. Then the feasibility of the dual-aptamers for constructing sandwich assay is validated *via* dynamic light scattering. This sandwich assay shows considerable sensitivity and specificity. The above results imply that the dual-aptamers have the potential to develop novel sensors for PP in clinical samples.

Pancreatic polypeptide (PP) is a 36 amino acid peptide produced and secreted by PP cells of the pancreas.[1] It was found to be associated with pancreatic neuroendocrine tumors (pNETs) since 1978[2] and later proven to be a specific marker of non-functional pancreatic neuroendocrine tumors (NF-pNETs).[3] NF-pNETs occupy more than half of the pNETs and have no specific hormone-related clinical syndromes.[4, 5] The rate of malignancy in NF-pNETs is ≥ 60%, and most patients present with metastatic disease at diagnosis.[6-8] Quantification of PP might contribute to the diagnosis and prognosis of NF-pNETs.[9]

In general, the basal PP in serum is ≤ 100 pmol[10] and associates with age and gender.[11] It would be sharply elevated (even to be 100-fold) in the presence of NF-pNETs with a sensitivity of 50 ~ 80 %.[12] The most common method to detect PP is radioimmunoassay (RIA) [13], whether in clinical medical laboratories (e.g., ARUP Laboratories[14] and Mayo Medical Laboratories[15]) or in-house assays[16]. RIA is a sensitive and specific technique but still has several disadvantages: radioactive materials, specialized equipment and a laboratory classified for handling radioactive assays.[17] Antibody-based enzyme-linked immunosorbent assay (ELISA) was another widely used protein detection assay in biomedical research and clinical diagnostics[18], however, there was no reported ELISA for PP until now. While LC-MS/MS-based method has also been developed for PP detection, this method still requires expensive equipment and complicated operation.[19] New strategies for PP detection were still urgently needed.

Aptamers are short, single stranded DNA or RNA developed by an *in vitro* process called SELEX (systematic evolution of ligands by exponential enrichment).[20] Due to the stable and cost-effective features, aptamers have been proven to be powerful molecular tools in biosensing and medical diagnoses in recent years.[21] The targets of aptamers range from ions, small molecules, proteins, bacteria, cells to tissues.[22] Meanwhile, aptamers have been incorporated with series of techniques, such as fluorescence, electrochemistry, colorimetry, surface enhanced Raman scattering (SERS) and surface plasmon resonance (SPR), etc. to construct sensors.[23] As affinitive reagents, aptamers show superiority to antibodies, particularly for the small size targets with poor immunogenicity.[24] Lots of aptamer-based sensors for small biomolecules have been widely designed, improving the detection of small biomolecules.[25] PP is a linear peptide with the molecular weight of 4.2 kD,[26] which is much smaller than many proteins. Aptamers might offer versatility and flexibility in sensor constructions for PP.

Compared to competitive assays, sandwich assays provide higher affinity and specificity to the targets because of two recognition elements.[27] The sandwich formats in ELISA conduce to minimize false positive results then reach an ultra-low detection limit.[28] However, developing sandwich ELISA is still problematic as limited analytes could provide enough immunogenic sites to generate antibodies for different epitopes.[29] Some researchers have chosen aptamers, which are accessible entirely synthetically *in vitro*, as alternatives in constructing sandwich-type sensors.[30] Dual-aptamers, i.e. a pair of aptamers which could bind to different epitopes of one target, were screened for several targets, such as thrombin, platelet-derived growth factor BB, H5Nx viruses, etc., and sensors were developed for sensitive and specific quantification.[31-33] Although split-aptamers were also used in constructing sandwich assays, they usually showed inactivity at physiological temperature and decreased affinity.[34, 35]

Herein, for the first time, high affinitive aptamers against PP were screened, and a sensitive and specific sandwich assay was developed *via* dual-aptamers. The aptamers were obtained through graphene oxide-based SELEX (GO-SELEX), an immobilization-free screening strategy.[36, 37] After 18 rounds of selections, three affinitive aptamers named 26_17, 10_13 and 5_13 were obtained.

Most importantly, 26_17 and 10_13 were proven to be the dual-aptamers for PP *via* fluorescence and dynamic light scattering assays. This dual-aptamers recognized PP sensitively and specifically, showing their value in PP detection.

Experimental Section

Materials and reagents. Pancreatic polypeptide (98%, purified by RP-HPLC) was purchased from ChinaPeptides Co., Ltd. (China). Graphene oxide (GO) was purchased from Nanjing XFNANO Materials Tech Co., Ltd. (China). Bovine serum albumin (BSA) and N-(2-Hydroxyethyl)piperazine-N'-(2-ethanesulfonic acid) (Hepes) were both purchased from Genview (USA). Human serum albumin (HSA) was purchased from Beijing Dingguo Changsheng Biotechnology Co., Ltd. (China). Hemoglobin (Hb) was purchased from Sangon Biotechnology Co., Ltd. (Shanghai, China). Glucagon (Glu) was purchased from Xi'an Plant Bio-engineering Co., Ltd. (China). Insulin (Ins) was purchased from Aladdin Industrial Corporation (China). 2× Power Taq PCR MasterMix was purchased from BioTeke Corporation (Beijing, China). Streptavidin agarose microbeads and NAP-5 columns were purchased from GE Healthcare Life Sciences (USA) for ssDNA generation experiments. SYBR® Gold (10,000 ×) and SYBR® Green I (10,000 ×) were both purchased from Invitrogen (USA). Gold chloride hydrate ($HAuCl_4 \cdot 4H_2O$) was purchased from Sinopharm Chemical Reagent Co., Ltd. (China). Human serum was purchased from Beijing Reanta Scientific and Technology Co., Ltd. (China). Acetonitrile (HPLC grade) was purchased from J&K Scientific Ltd (Beijing, China). The DNA pool was purchased from Takara Biotechnology (Dalian, China), and the other DNA sequences were synthesized, purified and characterized (ESI-MS) by Sangon Biotechnology Co., Ltd. (Shanghai, China). All of the chemical reagents were of analytical grade or higher, and were used as received without any further purification. Ultrapure water (18.2 MΩ.cm) was used throughout.

The selection of aptamers based on GO-SELEX. All the sequences used in SELEX were listed in Table S-1.

Mode I: The ssDNA pool was first incubated with PP at 37 °C for 2 h, then GO was added and the mixture was incubated for 25 min at 25 °C. Non-specific ssDNA would be adsorbed on GO and then removed by centrifugation at 17,700 g for 15 min. The supernatant containing ssDNA-target complexes were amplified by PCR. The ssDNA would be generated from PCR products by isolating and purifying, and then used as the pool for next round selection.

Mode II: The ssDNA pool was first incubated with GO at 25 °C for 25 min. After removed the supernatant through centrifugation at 17,700 g for 15 min, the precipitate was collected and resuspended in binding buffer, and then incubated with PP at 37 °C for 2 h. To get ssDNA-target complexes, the mixture was centrifugated and the supernatant was amplified and purified to generate ssDNA pool for next round selection.

Mode III: In order to obtain high specific aptamers, counter-SELEX was needed during the process of selection. The ssDNA pool was first incubated with counter-targets (BSA, HSA and Hb) at 37 °C for 1 h, then GO was added and the mixture was incubated for another 25 min at 25 °C. The non-specific ssDNA strands which bound to counter-targets would be removed by centrifugation at 17,700 g for 15 min. The precipitate was collected and resuspended in binding buffer, and then incubated with PP at 37 °C for 2 h. To get ssDNA-target complexes, the mixture was centrifugated and the supernatant was amplified and purified to generate ssDNA pool for next round selection.

In each Mode, ssDNA pools were first dissolved in 1× Binding Buffer (20 mM Hepes, 120 mM NaCl, 5 mM KCl, 2 mM MgCl2, pH=7.4) and denatured as follow: heated at 95 °C for 5 min, cooled down in ice-bath for 5 min and then remained in room temperature for 5 min. The amounts of GO were determined according to the optimal mass ratio of GO/ssDNA (Figure S-1). PCR was conducted in 10 parallel tubes with 50 μL reaction volume, which contained 2× Power Taq PCR MasterMix (25 μL), Forward Primer (10 μM, 2.5 μL), Biotin-Reverse Primer (10 μM, 2.5 μL), supernatants (2.5 μL) and ultrapure water (17.5 μL). The process of PCR was performed as follows: 94 °C for 10 min, followed by cycles of a rapid three-step PCR (30 s denaturation at 94 °C, 30 s annealing at 56.9 °C, 30 s extension at 72 °C), and finally extension at 72 °C for 7 min. The best cycle number was determined by 2 % agarose gel or 12 % native polyacrylamide gel electrophoresis, and 20 parallel tubes with the same components mentioned above were amplified by PCR again at the best cycle number to prepare pools for next round. All the PCR amplifications were carried out in Mastercycler pro (Eppendorf, Germany). Streptavidin agarose microbeads were used to capture dsDNA products from PCR through streptavidin-biotin reaction, and ssDNAs were generated and collected by denaturation (200 mM NaOH) and centrifugation at 2,500 g. After a desalting step by NAP-5 columns, the collected ssDNAs would be quantified by UV-visible measurements (Biospec-nano, Shimadzu) at 260 nm and used as the pools for next round.

Preparation of AuNP-aptamer. The AuNP-26_17 and AuNP-10_13 were prepared as follow: 5'-SH-26_17 (100 μM, 10 μL) or 5'-SH-10_13 (100 μM, 10 μL) was incubated with 5'-SH-Helper (100 μM, 10 μL) and 13 nm AuNPs (980 μL) at 4 °C for 16 h. Then PBS (30 mM, containing 300 mM NaCl, pH=7.4, 500 μL) was added and the solution was remained at 4 °C for 40 h. The excess DNA were removed by centrifugation at 13,300 g for 30 min at 4 °C, and the red precipitate would be washed twice with 1× Binding Buffer. The AuNP-26_17 or AuNP-10_13 were finally dispended in 1 × Binding Buffer (500 μL) and stored at 4 °C before using.

Feasibility of sandwich assay. Seven solutions (100 μL each) contained different components were prepared: a) 3 nM bare AuNPs; b) 3 nM AuNP-26_17; c) 3 nM AuNP-10_13; d) 3 nM AuNP-26_17 and 15 nM PP; e) 3 nM AuNP-

10_13 and 15 nM PP; f) 1.5 nM AuNP-26_17 and 1.5 nM AuNP-10_13; g) 1.5 nM AuNP-26_17, 1.5 nM AuNP-10_13 and 15 nM PP. The above solutions were incubated at 25 °C for 2 h, and the average particle size of each solution was measured by particle size analyzer (Zetasizer Nano ZS, Malvern).

Quantification of pancreatic polypeptide *via* sandwich assay. Under the optimal conditions, AuNP-26_17 (1.5 nM) and AuNP-10_13 (1.5 nM) were incubated with increasing concentrations of PP (0, 1, 2.5, 5, 7.5, 10, 15, 25 and 50 nM) at 25 °C for 2.5 h. After incubation, average particle size of each solution was measured. The specificity was characterized by incubating AuNP-26_17 (1.5 nM) and AuNP-10_13 (1.5 nM) with increasing concentrations (0, 1, 2.5, 5 and 10 nM) of different proteins (Glu, Ins, HSA, BSA and Hb). And the average particle size of each solution was measured after incubation.

Transmission electron microscope (TEM) characterization. Under the optimal conditions, AuNP-26_17 (1.5 nM) and AuNP-10_13 (1.5 nM) were incubated with increasing concentrations of PP (0, 5, 10, 15 nM) at 25 °C for 2.5 h. Then 20 μL of each sample was dripped onto the copper grid and dried by air. After that, the AuNPs were characterized by JEM-3010 (JEOL, Japan).

Results and discussion

***In vitro* selection of aptamers based on GO-SELEX.** The aptamers were developed based on a previously reported GO-SELEX strategy with three mode (Scheme 1).[38] Based on the combination of three different screen mode, DNA pools were enriched by PP gently to avoid losing the affinitive sequences. Mode I and Mode II were both positive selections, whereas Mode III consisted of positive and negative selections. Compared to Mode I, better affinity was needed to form target-ssDNA complexes in Mode II, as the ssDNA pools were adsorbed onto GO before being incubated with PP. In Mode III, ssDNA pools undergo the ordeals of counter-targets and GO before forming target-ssDNA complexes. Therefore, the selection stringency of the three modes was: Mode I < Mode II < Mode III. These three protocols were conducted alternately among the selection progress: Mode I was used to eliminate most non-specific sequences from random ssDNA and enrich the pool gently; Mode II was conducted to improve the stringency of selection; Mode III was carried out to obtain the specific and affinitive aptamers for PP. Optimal mass ratio of GO/ssDNA was also determined before selections, 0.6 μg/pmol was chosen according to the results in Figure S-1. Other details of the processes were listed in Table S-2.

After 18 rounds of selections, the enrichment assays were conducted (Figure S-2) and the PCR products of round 13th and 17th were subjected to high-throughput sequencing. As the sequencing results shown in Table S-3, there were fifty sequences with copy number ≥ 2. These sequences indicated non-significant homology (data not shown), but we still went on the study because the most abundant sequences identified in the selection products might not be necessarily the highest affinity aptamers.[39]

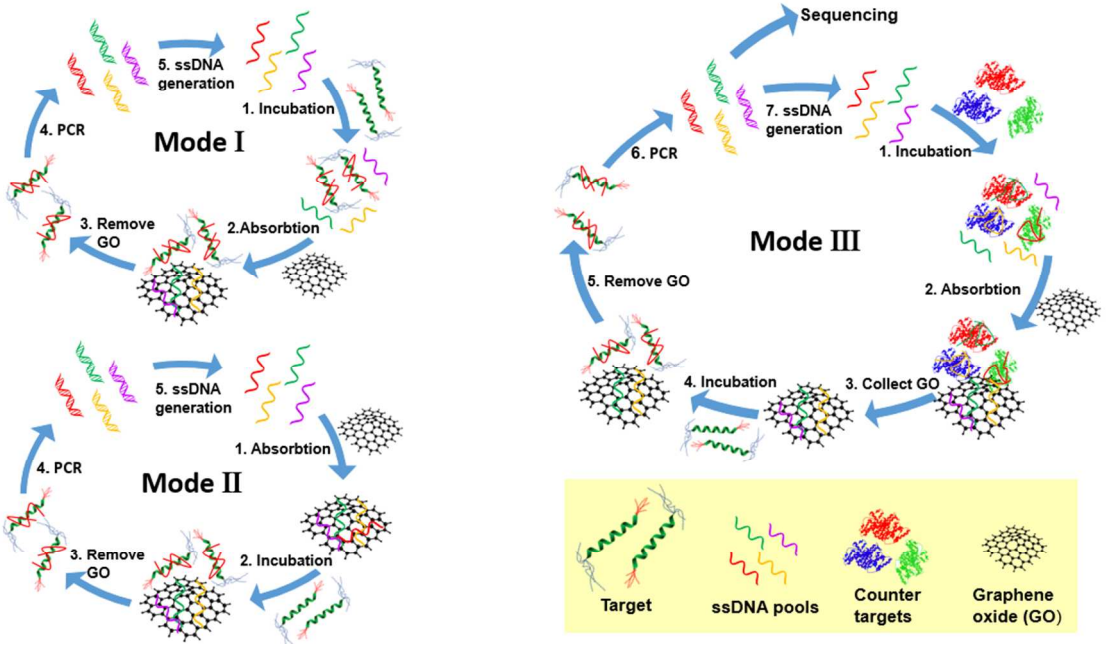

Scheme 1. Schematic illustration of GO-SELEX with three protocols. Mode I and II were both positive selections with different incubation orders. ssDNA pools were first incubated with PP in Mode I, but in Mode II they were firstly incubated with GO. In Mode III, positive and negative selections were integrated together to eliminate non-specific binding.

Characterization of aptamers. Purchase and characterizing of fifty 75 nt DNA oligomers would cost high and be a laborious task. To reduce cost and accelerate characterization, we cut down the primers and combined DNA

fluorescent dyes with microplate to construct two label-free strategies (Figure S-3): 1) SYBR® Green I-assisted fluorescence assay; 2) SYBR® Gold and GO-assisted fluorescence assay. Experimental details about the characterization of fifty primers-free sequences were shown in Section-6 in Supporting Information (SI). Only the sequences with significantly fluorescent signal changes of SYBR® Green I or SYBR® Gold can be the candidates, as the binding might change the secondary structures of DNA or create new complexes which could not be adsorbed onto GO. As the result, eight sequences (Table S-4) were picked out.

To eliminate false-positive results caused by non-specific adsorption of DNA dyes in the label-free strategies, eight candidate sequences were labelled with 5(6)-carboxyfluorescein (FAM) (Table S-5) and further explored by a GO quenching assay. To determine the K_d, PP were incubated with series concentrations of the sequences (10-200 nM) in dark, then GO were added with consistent mass ratio to ssDNA for adsorbing free ssDNA. After centrifugation, the fluorescence intensity of supernatants (F) would be measured. Negative controls, i.e. equivalent ssDNA and GO but without PP, were also conducted to determine the basal fluorescence (Fo), and the change of fluorescence (ΔF) was calculated through subtracting the Fo from F. As shown in Figure 1, there were four candidates which exhibited significant signals, but only three fit the binding saturation curves well ($Y=B_{max}X/(K_d+X)$, X represented the concentration of aptamers, Y represented the ΔF), named 26_17, 10_13 and 5_13. K_d and sequences of these aptamers were listed in Table 1. The K_d of 26_17, 10_13 and 5_13 were lower than 80 nM, indicating high affinities to PP. Secondary structures of these aptamers were also simulated and shown in Figure S-4.

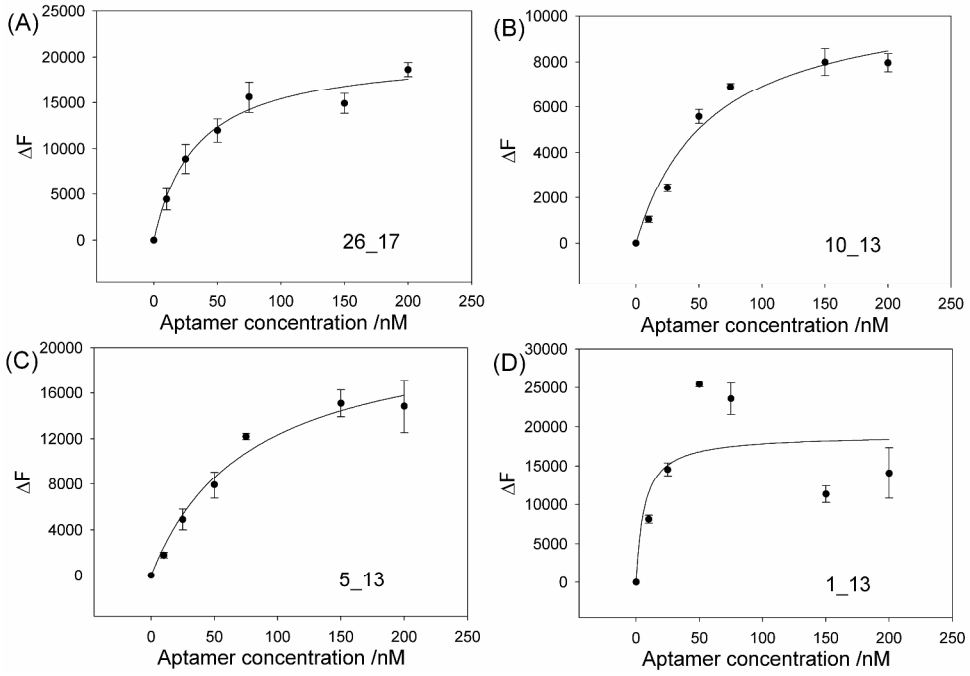

Figure 1. The affinity characterization assays. Binding saturation curves of selected aptamer to PP (A) 26_17; (B) 10_13; (C) 5_13; (D) 1_13. ΔF=F-Fo, where F and Fo represent the fluorescence intensities at 525 nm with or without PP, respectively. The error bars indicated the standard deviations of three parallel experiments.

Table 1. Sequences and K_d of selected aptamers.

Name	Sequence of random region (5'-3')	Length	K_d (nM)
26_17	GGCACCGCTGTTTTAGCCTCGGCTGAGACAAGGGC	35	33.15 ± 4.08
10_13	CGTGCAATGTCGAATGCATGAGCAAACATGGCGAT	35	58.81 ± 3.28
5_13	GGTTGATGTGCAACGAAGTAAGCATTAGCCAAAAG	35	77.39 ± 3.93
1_13	AGCCAAAACGGTGTTGAGGCCATGGCCTAACACAT	35	–

Here we hoped to obtain appropriate aptamer pairs which were suitable for constructing sandwich assays for PP. Therefore, a fluorescence quenching assays were conducted to pick out the sequences which could bind to different sites of PP. As shown in Figure 2A, two aptamers labelled with fluorophore or quencher were incubated with PP together. If the aptamers could bind to PP simultaneously, shorter distance between fluorophore and quencher would induce the decrease of fluorescence intensity. To pick out the pairs, three preferred aptamers were divided into three groups: 1) 26_17 and 10_13; 2) 26_17 and 5_13; 3) 10_13 and 5_13, and the effects of different labelling sites were also considered (Table S-6). As shown in Figure 2B, only the pair of 5'-BHQ1-26_17 and 3'-

FAM-10_13 showed significant reduce of fluorescence intensity when PP was present, whereas other pairs did not (Figure S-5). To determine whether this phenomenon was just a false-positive result induced by the hybridization between two aptamers, fluorescence intensities of 3'-FAM-10_13 only in the present of increasing 5'-BHQ1-26_17 or PP were also determined. As shown in Figure 2C, there were no significant changes in fluorescence intensity when PP was absent; meanwhile, PP would not influence the fluorescence of 3'-FAM-10_13 (Figure 2D), so the decreased signal in Figure 2B might be induced by the formation of sandwich complex. Results in Figure 2C also supported the hybridization prediction of 26_17 and 10_13 (Figure S-6), as there was not obvious hybridization between 26_17 and 10_13 under experimental conditions and the fluorescence intensity was invariant. Moreover, specificity of the dual-aptamers was also characterized. As shown in Figure 2E, there were no significant changes in fluorescence intensity in the present of control proteins, showing the high specificity of the dual-aptamers.

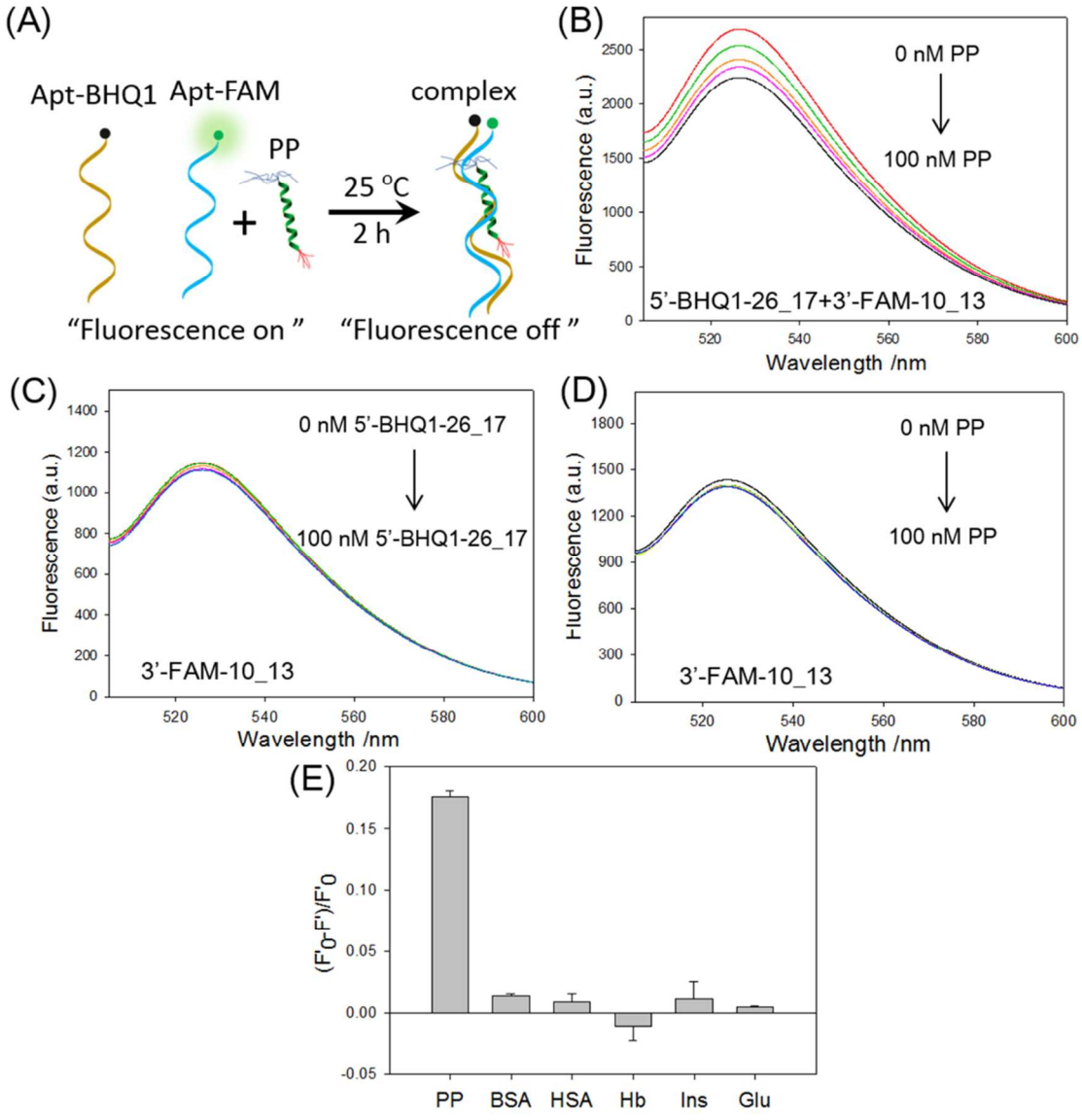

Figure 2. Fluorescence quenching assay to pick out the dual-aptamers. (A) Schematic illustration of fluorescence quenching assay; Apt-FAM: FAM-labelled aptamer; Apt-BHQ1: BHQ1-labelled aptamer; PP: pancreatic polypeptide. (B) Fluorescence spectra of 100 nM 3'-FAM-10_13 in the present of 100 nM 5'-BHQ1-26_17 and increasing concentration of PP (0, 10, 20, 50 and 100 nM). (C) Fluorescence spectra of 50 nM 3'-FAM-10_13 in the present of increasing concentration of 5'-BHQ1-26_17 (0, 10, 20, 50 and 100 nM). (D) Fluorescence spectra of 50 nM 3'-FAM-10_13 in the present of increasing concentration of PP (0, 10, 20, 50 and 100 nM). (E) Specificity investigation of the dual-aptamers. F' and F'0 represented the fluorescence intensities at 525 nm of 100 nM 3'-FAM-10_13 and 100 nM 5'-BHQ1-26_17 with or without 100 nM proteins (PP, BSA, HSA, Hb, Ins or Glu), respectively. The error bars indicated the standard deviations of three parallel experiments.

Dual-aptamers based sandwich assay for PP. Due to the strong localized surface plasmon resonance phenomenon, Au nanoparticles (AuNPs) have been incorporated with various methods (e.g. dynamic light scattering, col-

orimetry and SPR) [40-42] to develop sensitive analytical methods. Our group have succeeded in detecting adenosine *via* an AuNP-aptamer based dynamic light scattering (DLS) [43], showing a much lower limit of detection (LOD) compared to UV-visible spectrophotometry. Therefore, 5'-SH-26_17 and 5'-SH-10_13 (Table S-7) were immobilized on the surface of AuNPs (AuNP-26_17 and AuNP-10_13) to construct a sandwich-type DLS for PP. As shown in Scheme 2, AuNP-26_17 and AuNP-10_13 would disperse well in solution when PP was absent. However, larger clusters would exist in the presence of PP because AuNP-26_17 and AuNP-10_13 could bind to PP simultaneously, closing the distance of different AuNPs. This process could be characterized by DLS with clear signal changes.

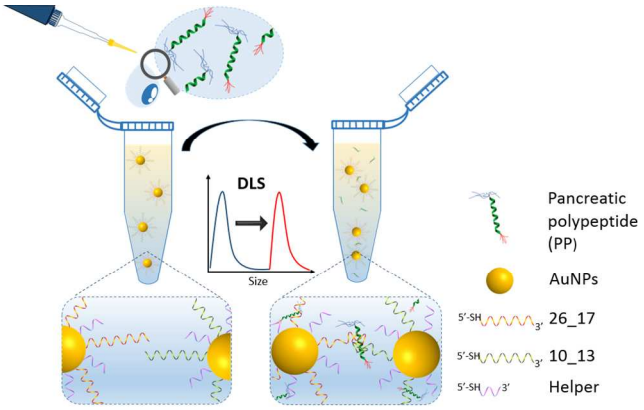

Scheme 2. Schematic illustration of the dual-aptamers based sandwich-type DLS assay for PP.

The feasibility of sandwich assay was first investigated. Red-shifts of UV-visible absorption spectra (Figure S-7, peak in 518nm to 521nm) and increases of hydrodynamic radio (Figure 3A, from about 7.0 nm to 9.0 nm) both indicated the successful modifications of 5'-SH-26_17 and 5'-SH-10_13 on the surface of AuNPs. Most importantly, only when AuNP-26_17, AuNP-10_13 and PP were present simultaneously did the hydrodynamic radio increased obviously (Figure 3A), demonstrating the sandwich mode among PP, AuNP-26_17 and AuNP-10_13. However, the presence of PP could not make clear difference in UV-visible spectrophotometry of the AuNP-26_17 and AuNP-10_13 mixture (Figure 3B), so that following experiments were conducted only through DLS.

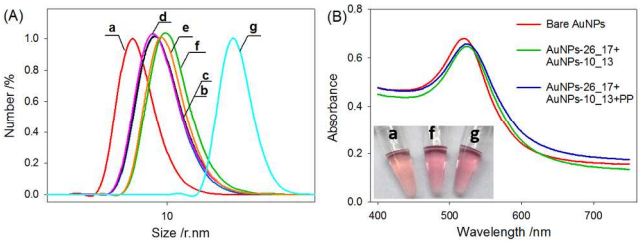

Figure 3. Feasibility of the sandwich assay. (A) The particle size of (a) bare AuNPs; (b)AuNP-26_17; (c) AuNP-10_13; (d) AuNP-26_17 + PP; (e) AuNP-10_13 + PP; (f) AuNP-26_17 + AuNP-10_13; (g) AuNP-26_17 + AuNP-10_13 + PP. Ordinate was normalized through dividing every data points by peak value. (B) UV-visible absorption spectra of (a) bare AuNPs, (f) AuNP-26_17 + AuNP-10_13 and (g) AuNP-26_17 +AuNP-10_13 + PP. Insert represented photos of the three samples.

To achieve a better performance, we investigated the effects of temperature, incubation time, ratio of aptamer to helper and ratio of AuNP-26_17 to AuNP-10_13 in this assay. As shown in Figure S-8, changes of hydrodynamic radio (ΔR) under different conditions would be compared to conduct the optimization, where ΔR was calculated by subtracting the basal hydrodynamic radio of AuNP-26_17 and AuNP-10_13 mixture from the hydrodynamic radio of AuNP-26_17/PP/AuNP-10_13 complexes. According to the results of DLS under different conditions, we chose 25 °C, 2.5 h, aptamer: helper = 1.5 and AuNP-26_17: AuNP-10_13 = 1 to conduct the quantitative detection of PP.

As shown in Figure 4A, ΔR increased significantly when AuNP-26_17 and AuNP-10_13 were incubated with increasing concentrations of PP under optimal conditions. It reached a plateau at the PP concentration of 15 nM, and showed a good linear response (changed from 1.43 ± 0.06 nm to 17.57 ± 0.02 nm) for PP in the range from 1 nM to 15 nM (insert in Figure 4A, R^2 = 0.9988). The LOD of this sandwich assay was 56 pM, which was calculated according to the standard equation y = 1.187x + 0.138 and the 3σ rule. Transmission electron microscope (TEM) images of AuNP-26_17 and AuNP-10_13 in the present of different concentrations of PP (Figure 4C) also supported the aggregation of AuNPs, as larger clusters existed with increasing concentrations of PP.

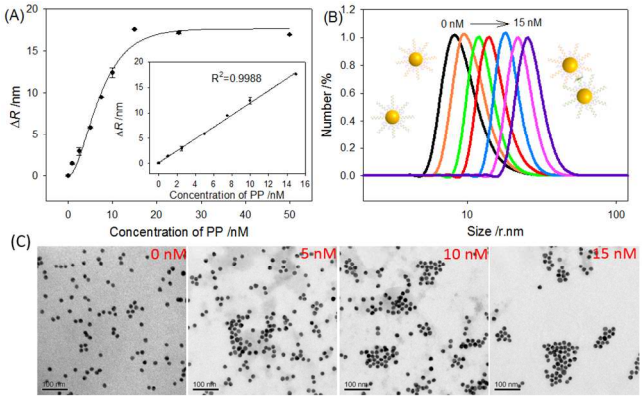

Figure 4. The LOD of sandwich assay. (A) Variance of the ΔR with increasing concentrations of PP (0, 1.0, 2.5, 5.0, 7.5, 10.0, 15.0, 25.0 and 50.0 nM), where the insert indicated the standard curve. The error bars indicated the standard deviations of three parallel experiments. (B) Particle size curves corresponding to the standard curve, ordinate was normalized through dividing every data points by peak value. (C) TEM images of AuNP-26_17 and AuNP-10_13 after addition of 0, 5, 10 and 15 nM PP.

Specificity of this strategy was also investigated by incubating AuNP-26_17 and AuNP-10_13 with increasing concentrations (0, 1, 2.5, 5 and 10 nM) of different proteins (Glu, Ins, HSA, BSA and Hb). As shown in Figure 5, ΔR

could only increase remarkably in the present of PP, demonstrating the high specificity of this sandwich assay.

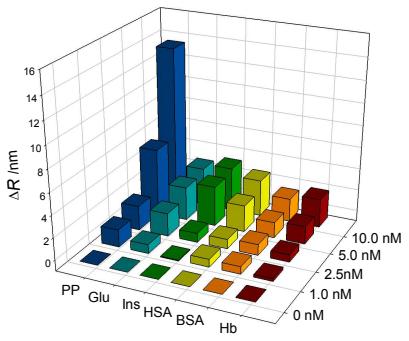

Figure 5. The specificity of PP to glucagon (Glu), insulin (Ins), human serum albumin (HSA), bovine serum albumin (BSA) and hemoglobin (Hb) in sandwich assay.

To evaluate the validity of this sandwich assay, recovery experiment was conducted in diluted human serum. Firstly, the standard equation of samples in diluted human serum was constructed (Figure S-9), and it would be used to determine the recovery. As listed in Table S-8, recovery of PP from diluted human serum was 90.7 ± 3.6% ~ 108.4 ± 1.6%, which demonstrated that this proposed method can be used for determination of PP in human serum samples.

Conclusions

In summary, we screened affinitive aptamers for PP and constructed a sensitive and specific dual-aptamers based sandwich assay. To the best of our knowledge, it was the first time to detect PP by aptamers. This aptamer-base sandwich assay showed several advantages: 1) environmental friendly: avoiding the use of radioactive materials; 2) operational friendly and time saving: experiments were conducted through easy incubations and measurements, while traditional RIA would take more than 3 days to get the results;[14] 3) considerable sensitivity and specificity: the LOD of this strategy in buffer was 56 pM, and control proteins (e.g. Glu, Ins, HSA, BSA and Hb) would not interfere so much. What's more, other sandwich assays based on different principles (e.g. SPR and electrochemistry) and amplified strategies (e.g. proximity ligation assay) could also be constructed through our dual-aptamers. To further reduce time cost and simplify assay procedures, dual-aptamers could be integrated with microfluidic technologies as well. We believed that the results in this paper would contribute to the development of novel biosensors for PP and have the potential in disease diagnosis.

ASSOCIATED CONTENT

Supporting Information. The Supporting Information is available free of charge on the ACS Publications website.

Experimental details of the SELEX, schemes and experimental details of two label-free characterization strategies, DNA sequences of candidate aptamers, simulated secondary structure of aptamers, experimental details and negative results of fluorescence quenching assays, simulation results of the hybridization between 26_17 and 10_13, synthesis and modifications of AuNPs, optimization of sandwich assay conditions in buffer, standard equation and recovery of PP in diluted human serum.

AUTHOR INFORMATION

Corresponding Author

* E-mail: yangxiaohai@hnu.edu.cn.
* E-mail: kmwang@hnu.edu.cn.

Author Contributions

‡These authors contributed equally.

Notes

The authors declare no competing financial interest.

ACKNOWLEDGMENT

This work was supported by the National Natural Science Foundation of China (21675047, 21375034, 21190040), the National Basic Research Program of China (2011CB911002).

REFERENCES

(1) Williams, J. A. Pancreatic polypeptide. *Pancreapedia: Exocrine Pancreas Knowledge Base* **2014**. DOI: 10.3998/panc.2014.4.

(2) Lonovics J.; Devitt P.; Watson L. C.; Rayford P. L.; Thompson J. C. Pancreatic polypeptide. *Arch. Sur.* **1981**, *116*, 1256-1264.

(3) Kanakis G.; Kaltsas G. Biochemical markers for gastroenteropancreatic neuroendocrine tumours (GEP-NETs). *Best Pract. Res. Clin. Gastroenterol.* **2012**, *26*, 791-802.

(4) Ramage J. K.; Ahmed A.; Ardill J.; Bax N.; Breen D. J.; Caplin M. E.; Corrie P.; Davar J.; Davies A. H.; Lewington V.; Meyer T.; Newell-Price J.; Poston G.; Reed N.; Rockall A.; Steward W.; Thakker R. V.; Toubanakis C.; Valle J.; Verbeke C.; Grossman A. B. Guidelines for the management of gastroenteropancreatic neuroendocrine (including carcinoid) tumors (NETs). *Gut* **2012**, *61*, 6-32.

(5) Alexakis N.; Neoptolemos J. P. Pancreatic neuroendocrine tumors. *Best Pract. Res. Clin. Gastroenterol.* **2008**, *22*, 183-205.

(6) Herrera M. F.; Åkerström G.; Angelos P.; Grant C. S.; Hoff A. O.; Pantoja J. P.; Johnston R. P.; Sahani D.V.; Wong R. J.; Randolph G. AACE/ACE disease state clinical review: pancreatic neuroendocrine incidentalomas. *Endocr. Pract.* **2015**, *21*, 546-553.

(7) Muniraj T.; Vignesh S.; Shetty S.; Thiruvengadam S.; Aslanian H. R. Pancreatic neuroendocrine tumors. *Dis. Mon.* **2013**, *59*, 5-19.

(8) Singh S.; Dey C.; Kennecke H.; Kocha W.; Maroun J.; Metrakos P.; Mukhtar T.; Pasieka J.; Rayson D.; Rowsell C.; Sideris L.; Wong R.; Law C. Consensus recommendations for the diagnosis and management of pancreatic neuroendocrine tumors: guidelines from a canadian national expert group. *Ann. Surg. Oncol.* **2014**, *22*, 2685-2699.

(9) Qiu W.; Christakis I.; Silva A.; Bassett Jr R. L.; Cao L.; Meng Q. H.; Grubbs E. G.; Zhao H.; Yao J. C.; Lee J. E.; Perrier N. D. Utility of chromogranin A, pancreatic polypeptide, glucagon, and gastrin in the diagnosis and follow-up of pancreatic neuroendocrine tumors in multiple

endocrine neoplasia type 1 patients. *Clin. Endocrinol.* **2016**, *85*, 400-407.
(10) Maxwell J. E.; O'Dorisio T. M.; Bellizzi A. M.; Howe J. R. Elevated pancreatic polypeptide levels in pancreatic neuroendocrine tumors and diabetes mellitus causation or association? *Pancreas* **2014**, *43*, 651-656.
(11) Brimnes D. M.; Rasmussen B. K.; Hilsted L.; Jensen R.; Hilsted J. Basal serum pancreatic polypeptide is dependent on age and gender in an adult population. *Scand. J. Clin. Lab. Invest.* **1997**, *57*, 695-702.
(12) Granberg D. Biochemical Testing in patients with neuroendocrine tumors. *Front. Horm. Res.* **2015**, *44*, 24-39.
(13) Sam A. H.; Sleeth M. L.; Thomas E. L.; Ismail N. A.; Daud N. M.; Chambers E.; Shojaee-Moradie F.; Umpleby M.; Goldstone A. P.; Le Roux C. W.; Bech P.; Busbridge M.; Laurie R.; Cuthbertson D. J.; Buckley A.; Ghatei M. A.; Bloom S. R.; Frost G. S.; Bell J. D.; Murphy K. G. Circulating pancreatic polypeptide concentrations predict visceral and liver fat content. *J. Clin. Endocrinol. Metab.* **2015**, *100*, 1048-1052.
(14) 2016 ARUP Laboratories, Laboratory Test Directory: Pancreatic Polypeptide, http://ltd.aruplab.com/tests/pub/0099436, accessed: 12, 2016.
(15) 1995-2016 Mayo Foundation For Medical Education And Research, Pancreatic Polypeptide in Plasma, http://www.mayomedicallaboratories.com/test-catalog/Overview/8014, accessed: 12, 2016.
(16) Ardill J. E. S. Circulating markers for endocrine tumors of the gastroenteropancreatic tract. *Ann. Clin. Biochem.* **2008**, *45*, 539-559.
(17) Burraco P.; Arribas R.; Kulkarni S. S.; Buchholz D. R.; Gomez-Mestre I. Comparing techniques for measuring corticosterone in tadpoles. *Curr. Zool.* **2015**, *61*, 835-845.
(18) Lequin R. M. Enzyme immunoassay (EIA)/enzyme-linked immunosorbent assay (ELISA). *Clin. Chem.* **2005**, *51*, 2415-2418.
(19) Escobar H.; Kushnir M. M.; Rockwood A. L.; Meikle A. W. High sensitivity measurement of pancreatic polypeptide and its variant in serum and plasma by LC-MS/MS. *Methods Mol. Biol.* **2016**, *1378*, 199-210.
(20) Ellington A. D.; Szostak J. W. *In vitro* selection of RNA molecules that bind specific ligands. *Nature* **1990**, *364*, 818-822.
(21) Famulok M.; Mayer G. Aptamers and SELEX in chemistry & biology. *Chem. Biol.* **2014**, *21*, 1055-1058.
(22) Ozalp V. C.; Kavruk M.; Dilek O.; Bayrac A. T. Aptamers: molecular tools for medical diagnosis. *Curr. Top. Med. Chem.* **2015**, *15*, 1125-1137.
(23) Famulok M.; Mayer G. Aptamer modules as sensors and detectors. *Acc. Chem. Res.* **2011**, *44*, 1329-1358.
(24) Gu C.; Lan T.; Shi H.; Lu Y. Portable Detection of Melamine in milk using a personal glucose meter based on an *in vitro* selected structure-switching aptamer. *Anal. Chem.* **2015**, *87*, 7676-7682.
(25) Feng C.; Dai S.; Wang L. Optical aptasensors for quantitative detection of small biomolecules: A review. *Biosens. Bioelectron.* **2014**, *59*, 64-74.
(26) Noelken M. E.; Chang P. J.; Kimmel J. R. Conformation and association of pancreatic polypeptide from three species. *Biochemistry* **1980**, *19*, 1838-1843.
(27) Rubio M. J.; Svobodová M.; Mairal T.; Schubert T.; Künne S.; Mayer G.; O'Sullivan C. K. β-Conglutin dual aptamers binding distinct aptatopes. *Anal. Bioanal. Chem.* **2016**, *408*, 875-884.
(28) Schweitzer B.; Roberts S.; Grimwade B.; Shao W.; Wang M.; Fu Q.; Shu Q.; Laroche I.; Zhou Z.; Tchernev V. T.; Christiansen J.; Velleca M.; Kingsmore S. F. *Nat. Biotechnol.* **2002**, *20*, 359-365.
(29) Vanderlugt C. L.; Miller S. D. Epitope spreading in immune-mediated diseases: implications for immunotherapy. *Nat. Rev. Immunol.* **2002**, *2*, 85-95.
(30) Csordas A. T.; Jørgensen A.; Wang J.; Gruber E.; Gong Q.; Bagley E. R.; Nakamoto M. A.; Eisenstein M.; Soh H. T. High-throughput discovery of aptamers for sandwich assays. *Anal. Chem.* **2016**, *88*, 10842-10847.
(31) Xu F.; Zhu Y.; Ma Z.; Zhao W.; Xu J.; Chen H. An ultrasensitive energy-transfer based photoelectrochemical protein biosensor. *Chem. Commun.* **2016**, *52*, 3034-3037.
(32) Wei L.; Wang X.; Wu D. J.; Li C.; Yin Y.; Li G. Proximity ligation-induced assembly of DNAzyme for simple and cost-effective colourimetric detection of protein with high sensitivity. *Chem. Commun.* **2016**, *52*, 5633-5636.
(33) Nguyen V. T.; Seo H. B.; Kim B. C.; Kim S. K.; C. Song S.; Gu M. B. Highly sensitive sandwich-type SPR based detection of whole H5Nx viruses using a pair of aptamers. *Biosens. Bioelectron.* **2016**, *86*, 293-300.
(34) Tang J.; Shi H.; He X.; Lei Y.; Guo Q.; Wang K.; Yan L.; He D. Tumor cell-specific split aptamers: target-driven and temperature-controlled self-assembly on the living cell surface. *Chem. Commun.* **2016**, *52*, 1482-1485.
(35) Lei Y.; Tang J.; Shi H.; Ye X.; He X.; Xu F.; Yan L.; Qiao Z.; Wang K. Nature-Inspired Smart DNA nanodoctor for activatable *in vivo* cancer imaging and *in situ* drug release based on recognition-triggered assembly of split aptamer. *Anal. Chem.* **2016**, *88*, 11699-11706.
(36) Park J. W.; Tatavarty R.; Kim D. W.; Jungb H. T.; Gu M. B. Immobilization-free screening of aptamers assisted by graphene oxide. *Chem. Commun.* **2012**, *48*, 2071-2073.
(37) Yang X.; Wang Y.; Wang K.; Wang Q.; Wan P.; Lin M.; Chen N.; Tan Y. DNA aptamer-based surface plasmon resonance sensing of human C-reactive protein. *RSC Adv.* **2014**, *4*, 30934-30937.
(38) Gu H.; Duan N.; Wu S.; Hao L.; Xia Y.; Ma X.; Wang Z. Graphene oxide-assisted non-immobilized SELEX of okdaic acid aptamer and the analytical application of aptasensor. *Sci. Rep.* **2016**, *6*, 21665.
(39) Ozer A.; Pagano J. M.; Lis J. T. New technologies provide quantum changes in the scale, speed, and success of SELEX methods and aptamer characterization. *Mol. Ther-Nucl. Acids.* **2014**, *3*, e183.
(40) Zheng T.; Pierre-Pierre N.; Yan X.; Huo Q.; A. Almodovar J. O.; Valerio F.; Rivera-Ramirez I.; Griffith E.; Decker D. D.; Chen S.; Zhu N. Gold nanoparticle-enabled blood test for early stage cancer detection and risk assessment. *ACS Appl. Mater. Interfaces* **2015**, *7*, 6819-6827.
(41) Zhou Y.; Dong H.; Liu L.; Xu M. Simple colorimetric detection of amyloid β-peptide (1–40) based on aggregation of gold nanoparticles in the presence of copper ions. *Small* **2015**, *11*, 2144-2149.
(42) Vaisocherová H.; Šípová H.; Víšová I.; Bocková M.; Špringer T.; Ermini M. L.; Song X.; Krejčík Z.; L. Chrastinová; O. Pastva; K. Pimková; M. D. Merkerová; J. E. Dyr; J. Homola. Rapid and sensitive detection of multiple microRNAs in cell lysate by low-fouling surface plasmon resonance biosensor. *Biosens. Bioelectron.* **2015**, *70*, 226-231.
(43) Yang X.; Huang J.; Wang Q.; Wang K.; Yang L.; Huo X. A one-step sensitive dynamic light scattering method for adenosine detection using split aptamer fragments. A*nal. Methods* **2011**, *3*, 59-61.

For TOC only

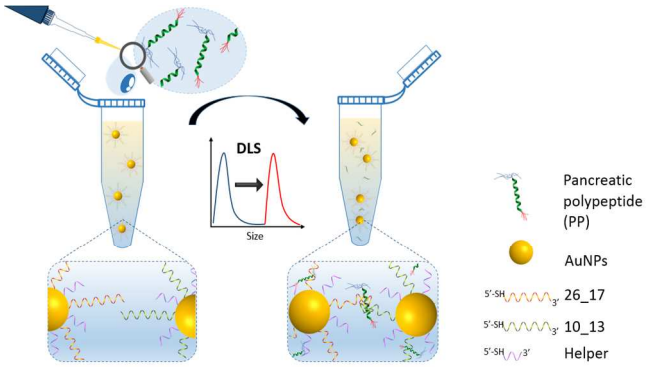
DLS
Size
Pancreatic polypeptide (PP)
AuNPs
5'-SH 3' 26_17
5'-SH 3' 10_13
5'-SH 3' Helper